Solving a Two-Scale Model for Vacuum Drying by Using COMSOL Multiphysics

Sadoth Sandoval- Torres [1*], Wahbi Jomaa[2], J-R. Puiggali[2]
[1]Instituto Politécnico Nacional. CIIDIR Unidad Oaxaca, México. CP. 71230, *ssandovalt@ipn.mx
[2]Université Bordeaux 1. Institut de mécanique et ingénierie de Bordeaux. Laboratoire TREFLE, Esplanade des Arts et Métiers 33405 Talence Cedex France.

Abstract: Drying of porous materials is characterized by the invasion of a gaseous phase replacing the evaporating liquid phase. Vacuum drying is an advanced method applied to oakwood to diminish discoloration, so understand its physics is a very important task.
In this work, a two-scale model is solved to simulate vacuum drying of oakwood. A two scale model describes the physics of wood-water relations and interactions with the vacuum dryer. Results provided important information about liquid and gas phase transport in wood. Water vapor and dry-air dynamics in the chamber were simulated linking large scale (dryer) and macroscale (wood) changes. We analyses results at 60–100 bar and 250–300 mbar both at 70°C. The physics-based one-dimensional model was solved by using the COMSOL's coefficient form and the global equations tool in COMSOL. The numerical results and experimental measures provide some confidence in the proposed model.

Keywords: Vacuum drying, Drying physics. Coupled model, Comsol multiphysics©.

1. Introduction

Vacuum drying of wood offers reduced drying times and higher end-product quality compared with others conventional drying operations [1]. The reduction of the boiling point of water at low pressure facilitates an important overpressure to enhance moisture evacuation. It is well known drying is a critical step in manufacturing timber products and is one of the most pressing issues in wood industry since there is a growing emphasis on high quality dried lumber because customers demand timber products which are defect free [2].

Benefits of vacuum atmospheres include the reduced drying times, recovery of vapors, and a higher end-product quality [1]. Operating at low pressures the boiling point of water is reduced, which in turn enables an important overpressure that drives moisture efficiently [3]. For some wood species like oak that cannot be dried at high temperature conditions, vacuum drying offers the possibility to avoid collapse and discoloration [4].

According to Turner [5], in drying modeling, different approaches can be adopted. Nevertheless, a complete formulation can be adopted from computational models based on nonlinear conservation laws. These models are called physics-based models. A complete description was published by Whitaker [6]. In this work a one-dimensional problem is solved in COMSOL multiphysics 3.5a. This package provides a number of application modes that consist on predefined templates and user interfaces to solve systems of partial and ordinary equations.

2. Mathematical formulation

The approach proposed by Whitaker [6] and Perré [3] was followed in this work. Mass and energy conservation relations are written for liquid water, water vapor and for the gaseous mixture (water vapor + air). A set of macroscopic equations were obtained, where the flux of the different components are described using different transport coefficients and driving forces. The two scale formulation considers the dryer scale and material scale changes. The scales are coupled by considering the evaporative flux and vacuum pump suction.
Porous media (wood sample) consists of a continuous rigid solid phase which contains a liquid phase (free water), bound water, and a continuous gaseous phase which is assumed to be a perfect mixture of vapor and dry air.

A mathematical description is developed on a continuum approach, where the macroscopic partial differential equations are achieved by volume averaging of the microscopic conservation laws. The method of volume averaging is a technique used to rigorously derive continuous macroscopic equations from the description of the problem at a microscopic

scale for multiphase systems. This method allows change the scale of description of the problem. The value of any physical quantity at a point in space is given by its average value on the averaging volume (AV) centered at this point [6]. The phase average is defined by

$$\bar{\psi} = \frac{1}{V}\int_v \psi \cdot dV$$

and the intrinsic phase average i by

$$\bar{\psi}^{i} = \frac{1}{V_i}\int_{v_i} \psi \cdot dV$$

Two problems related to wood drying simulations are usually the approximations made to the complete models and the question of their validity. Additional assumptions are required for proper evaluation of all simplifications. Then, the next hypothesis must be established in this work:

- European Oakwood have a very low permeability, this fact allows us to consider the gravitational effects are negligible.
- We consider that temperature and pressure in the dryer are homogeneous
- Vapor is an ideal gas both in the material and in the dryer.
- Thermodynamic equilibrium, so average temperatures for each phase are the same, and partial vapor pressure is at the equilibrium.
- No chemical reaction or shrinking occurs during wood drying.
- Lack of heat and mass losses assuming ideal isolation [20].

Then, we can write:

$$\overline{T}_v = \overline{T}_f = \overline{T}$$

$$P_v = a_w \cdot P_v^{sat}$$

During drying, free water is firstly evacuated, in this way saturation tends to zero. When saturation is zero, bound water is in its maximal concentration. In wood technology this point is referred as the fiber saturation point (fsp). For European oakwood (Quercus pedonculae) this point is 0.4 approximately.

Porosity can be defined as follow:

$$\varepsilon = \frac{Volume of\ pores}{Total Volume}$$

Compressibility effects in the liquid phase are neglected.

$$\rho_l^l = \rho_l = cste$$

Gas phase is considered as an air/water vapor ideal mixture, then:

$$\bar{\rho}_i^{g} = \frac{m_i \bar{P}_i^{g}}{R\bar{T}}$$

$$\bar{P}_g^{g} = \bar{P}_a^{g} + \bar{P}_v^{g}$$

$$\bar{\rho}_g^{g} = \bar{\rho}_a^{g} + \bar{\rho}_v^{g}$$

Where $\bar{\rho}_i^{g}$ is the intrinsic average density of each phase i, $\bar{P}_i^{g}$ is the pressure of the *i* specie in the phase g, and $\bar{T}$ the temperature. The molar mass is mi and R is the ideal gas constant.

3. Scale of the material

3.1 Transport of the liquid phase in wood.

In figure 1, we show the experimental configuration.

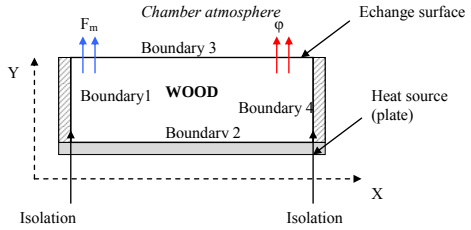

Figure 1. Experimental configuration.

Free water transport is explained by Darcy's law. The velocities of the gaseous and liquid phases are, respectively, expressed using the generalized Darcy's:

$$\bar{V}_l = -\frac{\bar{\bar{k}}\cdot\bar{\bar{k}}_{rl}}{\mu_l}\cdot(\nabla \bar{P}_l^{l} - \rho_l \cdot g)$$

$$\bar{V}_g = -\frac{\bar{\bar{k}}\cdot\bar{\bar{k}}_{rg}}{\mu_g}\cdot(\nabla \bar{P}_g^{g} - \rho_g \cdot g)$$

Capillary pressure is defined as:

$$\bar{P}_l^{l} = \bar{P}_g^{g} - Pc$$

$$P_c = 56.75\times10^3(1-S)\exp\left(\frac{1.062}{S}\right) \text{ (Pa)}$$

Capillary pressure is a driving force during capillary phase (free water evacuation). In fact above the fps only capillary and bulk flow may be considered imperative. We can write the flux of free water as:

$$\rho_l V_l = \rho_l \frac{\underline{\underline{k}}_{rl}\cdot k}{\mu_l}\cdot\nabla P_c - \rho_l \frac{\underline{\underline{k}}_{rl}\cdot k}{\mu_l}(\nabla \bar{P}_g^{\,g} - \rho_l g)$$

3.2. Transport of the vapor phase in wood

We consider water vapor and air mobility depends on pressure and concentration gradients of the gaseous phase. Then, for the mass flux of air and water vapor we write:

$$\bar{\rho}_v^{\,g}\bar{V}_v = \bar{\rho}_v^{\,g}\frac{\underline{\underline{k}}_{eq}\cdot k}{\mu_g}\cdot\nabla \bar{P}_g^{\,g} - \bar{\rho}_g^{\,g}\underline{\underline{D}}_{eq}\cdot\nabla C$$

$$\bar{\rho}_a^{\,g}\bar{V}_a = \bar{\rho}_a^{\,g}\frac{\underline{\underline{k}}_{eq}\cdot k}{\mu_g}\cdot\nabla \bar{P}_g^{\,g} - \bar{\rho}_g^{\,g}\underline{\underline{D}}_{eq}\cdot\nabla C$$

Where $\underline{\underline{k}}_{eq}$ and $\underline{\underline{D}}_{eq}$ are the equivalent permeability and the diffusion coefficient respectively; with these parameters the perturbations in the convective and diffusive dusty transport are considered.

A phenomenological approach can explain bound water flows in wood:

$$J_b = -\bar{\rho}_s\underline{\underline{D}}_b\cdot\nabla W_b - \bar{\rho}_s\underline{\underline{D}}_{bt}\cdot\nabla\bar{T}$$

Below FSP, the moisture is considered bound to the cell wall and, therefore, bound water diffusion can be considered to be the predominant mass transfer mechanism.

During drying, free water (liquid water), water vapor and bound water evaporates and leave the board, so the global balance is expressed by:

$$\frac{\partial W}{\partial t} + \nabla\cdot\left\{\frac{1}{\rho_s}\left(\rho_l\bar{V}_l + \bar{\rho}_v^{\,g}\bar{V}_l + Jb\right)\right\} = 0$$

For energy:

$$\overline{\rho Cp}\frac{\partial\bar{T}}{\partial t} + \left[(\rho_l\bar{V}_l Cp_l + J_b Cp_l + \bar{\rho}_a^{\,g}\bar{V}_a Cp_a + \bar{\rho}_v^{\,g}\bar{V}_v Cp_v)\right]\nabla\bar{T} - \left(\overline{\rho_b V_b}\cdot\nabla h_b\right) + \left(h_v K\right) + (h_v + h_b)K_b - \nabla\cdot(\underline{\underline{\lambda}}\cdot\nabla\bar{T}) = 0$$

2

4. Scale of the dryer

The dry-air and water vapor balance in the chamber are equations derived by assuming the pressure and temperature fields within the chamber are homogeneous. Using a control volume that includes the surfaces of the wood sample, the mass fluxes, and the vacuum pumping, we can derivate the conservation equations for the vacuum chamber:

$$\frac{d\rho_a^{ch}}{dt} = -\rho_a^{ch}\frac{q_{pump}}{V_{ch}} + \rho_a^{atm}\frac{q_{leak}}{V_{ch}}$$

for the dry-air

$$\frac{d\rho_v^{ch}}{dt} = -\rho_v^{ch}\frac{q_{pump}+q_{cond}}{V_{ch}} + \rho_v^{atm}\frac{q_{leak}}{V_{ch}} + F_m\frac{A}{V_{ch}}$$

For the water-vapor

Pressure in the chamber is computed according to the ideal gas law.

5. Boundary conditions

The pressure at the external drying surfaces is fixed at the atmospheric pressure Pch (Pressure of the chamber). Recalling that one of the primary variables used for the computations is the averaged air density.

We impose a Dirichlet boundary condition for the air flux equation. The Dirichlet boundary condition has been modified to form an appropriate non-linear equation for this primary variable [7]. For moisture fluxes, we consider equilibrium between water vapor at the wood surface and the vapor pressure in the chamber. Water vapor depends on pressure since to compute vapor density the ideal gas law is used. In the chamber atmosphere, we established that a mixture water–vapor/dry-air exists, that depends on dryer atmosphere temperature.

For energy fluxes we establish that temperature in the wood surface is in equilibrium with the chamber temperature.

Then, we can write:

$P_a^g = P_a^{chamber}$ For dry air

$\rho_v^g = \rho_v^{chamber}$ For water vapor

6. Implementation in COMSOL

To solve the set of equations, we have used the commercial solver COMSOL Multiphysics 3.5a. COMSOL offers solvers with a very high level of performance. Globally, COMSOL offers three possibilities to write the equations: (1) by using a template (Fick's law, Fourier's Law), (2) by using the coefficient form (for mildly nonlinear problems), and (3) by using the general form (for most nonlinear problems). We have written differential equations in the coefficient form. The equations were solved by using an unsymmetric-pattern multifrontal method. We have used a direct solver for sparse matrices (UMFPACK), which involve much more complicated algorithms than for dense matrices. The main complication is due to the need for efficient handling the fill-in in the factors L and U.

An Arbitrary Lagrange–Eulerian (ALE) formulation was applied. The sparse matrix A factorized by UMFPACK can be real or complex, square or rectangular, and singular or nonsingular (or any combination).

The mesh consists of 135 elements (1-D), time stepping is 0.1 (0 to 20 s of solution), 5 (20 to 100 s of solution, 100 (100 to 10000s of solution), and 10 (10000 to 100000s of solution). Several grid sensitivity tests were introduced to determine the sufficiency of the mesh scheme and to insure that the results are grid independent. We have established a maximum element size of 2e-4.

7. Results

We have written the partial differential equations (material scale) in the general form. The two ordinary differential equations (dryer scale) were introduced by considering the pump suction (0.0027 m3/s). To add the ODE's equation for the dryer scale, we have chosen a global equation format.

Fig. 2 shows predicted and experimental results for the vacuum drying at 70°C and 60–100 mbar of pressure. One can observe that the model is able to predict the kinetics of drying. In the same figure one can see that computed pressures inside dryer have a good agreement with the experimental data. The differences in the drying kinetic can be explained by variation of values in permeability, capillary pressure and transfer coefficients of water vapor, since they can vary (wood heterogeneity).

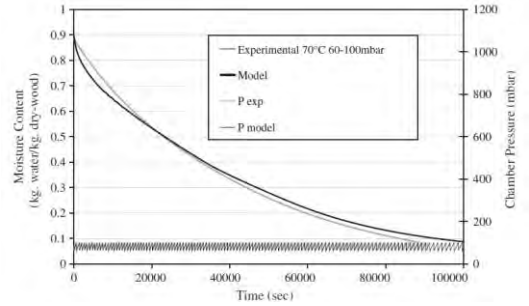

Figure 2. Comparison between vacuum drying kinetics: experimental and model. 70°C and 60–100 mbar.

Fig. 3 shows the experimental drying kinetics at 70°C and 250–300 mbar and simulation results. In both experimental observation and simulation one can see a more important drying time compared to drying time at 60-100 mbar. This may be explained by a lower overpressure generated between the heart and its wood surface. It is well known that overpressure generated in wood accelerates the mass transfer in the material.

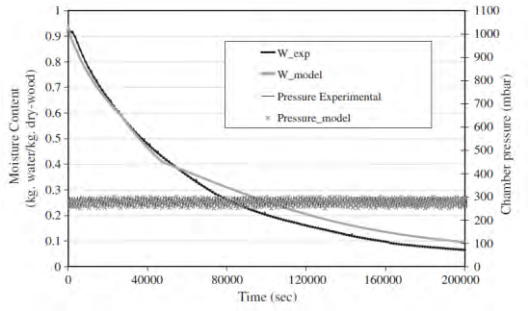

Figure 3. Simulation results versus experimental kinetics. 70°C 250–300 mbar.

Increase of permeability decreases the temperature gradients, but increases the diffusive coefficients. The relative change of temperature gradients at high temperatures is small so that the effect of decreasing the permeability on the

diffusive coefficient prevails and drying rates are reduced. At lower temperatures (our case), the relative change of the temperature gradients becomes higher, and this counterbalances the increase of the diffusive coefficients. The temperature curves are not smooth, and this can be explained by both the functions utilized for calculation and aspiration/no aspiration dynamics of the pump.

The pump works at two regimes: passive and active (on and off). The external vacuum reduces the required temperature for evaporation. The effective vapor transport increases with decreasing distance from the surface.
When comparing the mass fluxes, it can be identified two phases or regimes of drying (one active and other one passive).
Fig. 4 shows such fluxes, for a vacuum drying experiment at 70°C and 250–300 mbar of pressure. The drying phases produces natural oscillations at the surface temperature, since during active phase (pump suction) a temperature shut exist due to evaporation, and during the passive phase a re-homogenization is developed. Then, during the active phase mass flow is more important due to the operation of the pump, so there is a pressure drop in the enclosure and consequently faster evaporation in the surface of the material. Compared with the passive regime, during the active regime the evaporation is less intense since the pump is stopped, what causes an increase in the pressure chamber and a moisture homogenization, visible at the surface.

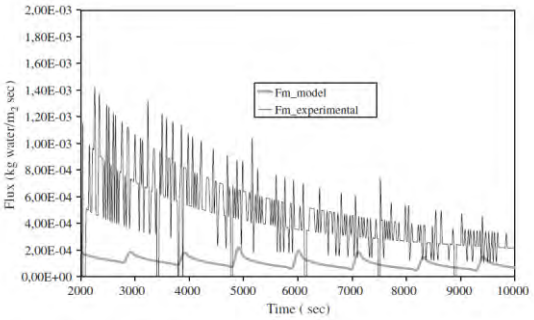

Figure 4. Mass fluxes during vacuum drying.

8. Conclusions

We have solved a model for vacuum drying of wood. This solution takes into account the two scale of this process: the dryer scale and the material scale. The numerical solution appears to be satisfactory. A good agreement between experimental results and those of the simulation is assessed. It is interesting to see how this model allows distinguishing the fast drying phase (active phase) from the passive phase (the homogenization period). The coupling between the wood material (product) and dryer (process) is also respected, this coupling is ensured by the boundary conditions imposed in our 1D simulations. These simulations are relevant because they represent quite well the experimental curves in terms of average kinetic, overall behavior of the dryer and liquid and vapor mobility.

9. References

[1] B.J. Ressel, State-of-the-art on vacuum drying of timber, in: Proceedings of the Fourth International IUFRO Wood Drying Conference, Rotorua, New Zealand, 1994, pp. 255–262.
[2] L. Cai, A. Koumoutsakos, S. Avramidis, on the optimization of a RF/V kiln drying schedule for thick western hemlock timbers, J. Inst. Wood Sci. 14 (6) (1998) 283–286.
[3] P. Perré, I.W. Turner, A dual-scale model for describing drier and porous medium interactions, AIChE J. 52 (9) (2006) 3109–3117.
[4] W. Jomaa, O. Baixeras, Discontinuous vacuum drying of oak wood: modelling and experimental investigations, Drying Technol. 15 (9) (1997) 2129–2144.
[5] I.W. Turner, P. Perré, Vacuum drying of wood with radiative heating: II. Comparison between theory and experiment, AIChE J. 50 (1) (2004) 108–118.
[6] S. Whitaker, The Method of Volume Averaging, Kluwer Academic Publishers, Dordrecht, 1999.
[7]. S. Sandoval Torres. Thèse de Doctorat. Université Bordeaux 1 – France. 2008.

10. Acknowledgements

To Instituto Politécnico Nacional, CIIDIR Oaxaca. México. Thanks so much to COFAA-IPN